Turkish Journal of Electrical Engineering & Computer Sciences

http://journals.tubitak.gov.tr/elektrik/

Research Article

Turk J Elec Eng & Comp Sci
(2015) 23: 522 – 538

doi:10.3906/elk-1301-170

Tracking control of elastic joint parallel robots via state-dependent Riccati equation

Sinan KILIÇASLAN*
Department of Mechanical Engineering, Faculty of Engineering, Gazi University, Ankara, Turkey

Received: 23.01.2013 • **Accepted:** 14.04.2013 • **Published Online:** 23.02.2015 • **Printed:** 20.03.2015

Abstract: In this study, a methodology for the tracking control of parallel robots having elastic joints based on the state-dependent Riccati equation is developed. Structural stiffness and damping characteristics of the joints are modeled as torsional springs and dampers, respectively. First an open-tree system is obtained by cutting some joints of the parallel robot open and its dynamic equations are written. Closed loops are then represented as constraint equations. The first and second derivatives of dependent (unactuated) joint variables are expressed in terms of independent (actuated) joint variables by making use of the constraint equations. Taking the independent joint variables, the actuator variables, and their first derivatives as state variables, the dynamic equations are represented in state-dependent coefficient form. Finally, state-dependent Riccati equation tracking control is presented. A 2-RRR planar parallel robot is taken into consideration as an example to illustrate the effectiveness of the state-dependent Riccati equation method for the control of parallel robots having elastic joints.

Key words: Elastic joint robot, parallel robot, trajectory tracking, state-dependent Riccati equation, optimal control

1. Introduction

Parallel manipulators have closed-loop configurations. Therefore, they have better positional accuracy and better heavy load capacity than serial manipulators. Flight simulators, precise machine tools, micro mechanisms, haptic devices, etc. can be given as examples of the application areas of these manipulators. On the other hand, these manipulators have workspace limitations and complexities in their dynamics and control. Therefore, parallel manipulators have attracted the attention of many authors in the past decades.

It was shown in an experimental study that the principle effect on manipulator elasticity results from the joint elasticity [1]. Moreover, it was shown in an empirical study that when joint elasticity is neglected in manipulator dynamics, the performance of the manipulator decreases [2]. Therefore, joint elasticity should be included in the modeling to achieve better positional accuracy.

In recent years, the state-dependent Riccati equation (SDRE) technique has been effectively used in the design of nonlinear controllers, observers, and filters due to its flexible design property, simplicity, and real-time implementation capability. The SDRE method received considerable attention after the studies of Cloutier et al. [3] and Mracek and Cloutier [4]. The capabilities of the method were overviewed by Cloutier and Stansbery [5]. Shamma and Cloutier [6] studied the existence of SDRE stabilizing feedback. Recently, detailed literature on the method was reviewed by Cimen [7,8]. The method has been used in a class of practical applications having

*Correspondence: skilicaslan@gazi.edu.tr

nonlinear structures such as autopilot design, integrated guidance and control design, satellite and spacecraft control, control of small autonomous helicopters, robotics, ducted fan control, control of aeroelastic systems, process control, control of systems with parasitic effects, control of artificial human pancreas, control of oil tanker motion, optimal administration of chemotherapy in cancer treatment, and various benchmark problems.

Although the SDRE method has been used in a class of practical applications having nonlinear structures, application of the method for the control of robots is scarce in the literature. Erdem and Alleyne [9], Terashima et al. [10], Watanabe et al. [11], Nekoo [12], Cree and Damaren [13], Shawky et al. [14,15], and Fenili and Balthazar [16] considered serial manipulators in their studies and did not consider joint elasticities. Korayem et al. [17] considered joint elasticities in the context of a serial manipulator. Therefore, application of the SDRE method for the control of robots having elastic joints for both serial and parallel manipulators needs to be investigated.

One method for the control of manipulators having elastic joints is analytical inverse dynamics control [18–20]. In this method, control torques are represented in terms of end-effector variables. The other method for control of manipulators having elastic joints is the singular perturbation method [18,21]. In this method, dynamics of the manipulator are divided into fast and slow dynamics corresponding to the dynamics of the elastic joints and the rigid manipulator, respectively. First, the fast dynamics are neglected. Then, by assuming slow variables as constant, fast dynamics are recalculated on a separate time scale for correction.

Hybrid force and motion control of serial manipulators having elastic joints were investigated by Ider [22], Hu and Vukovich [23], and M and Wang [24]. Adaptive control strategies were used by Chatlatanagulchai and Meckl [25], Jiang and Higaki [26], Yoo [27], Yena and Chang [28], and Fateh [29] for the control of elastic joint serial manipulators.

There are very few contributions in the literature for the control of parallel manipulators in the presence of elastic joints. Ider and Korkmaz [30] studied the trajectory tracking control of a flexible joint parallel manipulator by using the analytical inverse dynamics method. The major drawback of the inverse dynamics approach is the large real-time computational burden due to the complex inverse dynamics calculations.

Survey papers related to dynamics and control of manipulators with elastic joints have been written by Ozgoli and Taghirad [31] and Dwivedya and Eberhard [32].

As seen from this literature review, studies on the control of parallel robots having elastic joints are very scarce. Its flexible design property, simplicity, and real-time implementation capability make the SDRE method preferable compared to other control techniques. In this work, performance of the SDRE method for the tracking control of parallel robots having elastic joints is investigated. To the best of the author's knowledge, this is the first work in which the SDRE method is implemented on the control of parallel robots having elastic joints. Structural stiffness and damping characteristics of the joints are modeled as torsional springs and dampers, respectively. First, a constrained (closed-loop) system is transformed into an unconstrained (open-tree) system by disconnecting arbitrary unactuated joints and the dynamic equations of the unconstrained system are written. The constraint equations corresponding to the closed loops are then written. Using the constraint equations, the first and second derivatives of the dependent (unactuated) joint variables are represented in terms of independent (actuated) joint variables. By taking the independent joint variables, the actuator variables, and their first derivatives as state variables, the dynamic equations are represented in state-dependent coefficient form. Finally, the SDRE tracking control method is presented.

This study consists of 5 sections. Section 2 gives the mathematical description of the parallel robots with elastic joints. SDRE tracking control is presented in Section 3. In Section 4, a 2-RRR planar parallel robot

is taken into consideration as an example to illustrate the effectiveness of the SDRE method for the control of parallel robots having elastic joints. Finally, Section 5 gives the concluding remarks of this study.

2. Mathematical description of the flexible joint parallel manipulators

An n-degree of freedom constrained (closed-loop) system can be transformed into an unconstrained (open-tree) system by disconnecting arbitrary unactuated joints. If the degree of freedom of the unconstrained system is m, then m – n constraint equations are written. Assume that the manipulator joint variables of the unconstrained system are denoted as follows.

$$q = \begin{bmatrix} \theta_1 \\ \vdots \\ \theta_m \end{bmatrix} \tag{1}$$

It can be divided into 2 subvectors as independent (primary) and dependent (secondary) joint variables and they are represented as

$$q = \begin{bmatrix} q_p \\ q_s \end{bmatrix}, \tag{2}$$

where $q_p \in \Re^n$ is the vector of the independent joint variables corresponding to the actuated joints and $q_s \in \Re^{m-n}$ is the vector of the dependent joint variables corresponding to the unactuated joints.

Elastic members of the drive trains, e.g., thin shafts, harmonic drives, and couplings, cause flexibility at the independent (driven) joints. The flexible transmission in an independent flexible joint is modeled as a torsional spring with stiffness k_i and a torsional damping with damping coefficient d_i. Let the actuator variables of the driven joints be denoted as

$$\varphi = \begin{bmatrix} \varphi_1 \\ \vdots \\ \varphi_n \end{bmatrix}, \tag{3}$$

where each φ_i is the rotor angle divided by the gear ratio r_i of the corresponding actuated joint. Therefore, the elastic transmission between the links and the actuators introduces extra degrees of freedom, which means that the rotor of each actuator is modeled as a fictitious link. Thus, the overall system has 2n degrees of freedom although there are only n actuators.

The m – n constraint equations can be expressed at position level as

$$\psi_i(\theta_1, \ldots, \theta_m) = 0 \quad i = 1, \ldots, (m-n). \tag{4}$$

Differentiation of Eq. (4) gives

$$J(q)\,\dot{q} = 0, \tag{5}$$

where $J \in \Re^{(m-n)\times m}$ is the constraint Jacobian matrix, given as

$$J_{ij} = \frac{\partial \psi_i}{\partial \theta_j}. \tag{6}$$

In order to simplify the equations of motion of the parallel manipulator and make them more appropriate for analysis and control, some assumptions were made, as stated by Spong [18].

Assumption 1 The rotor kinetic energy essentially results from its own rotation since the gear ratio is sufficiently large.

Assumption 2 The rotor/gear inertia is symmetric about the rotor axis of rotation so that the gravitational potential of the system and the velocity of the rotor center of mass are independent of rotor position.

Therefore, the inertia and gravitational coupling terms between the joint and actuator variables vanish. Thus, unconstrained system equations of motion of the parallel manipulator can be written as

$$M(q)\ddot{q} + C(q,\dot{q})\dot{q} + G(q)q_p + F_d + F_k - J^T(q)\lambda = 0, \tag{7}$$

$$I^r\ddot{\varphi} - D(\dot{q}_p - \dot{\varphi}) - K(q_p - \varphi) = u, \tag{8}$$

where $M(q) \in \Re^{m\times m}$ is the generalized mass matrix, $C(q,\dot{q}) \in \Re^{m\times m}$ is the matrix corresponding to the generalized Coriolis and centrifugal force vector, and $G(q) \in \Re^m$ is the matrix corresponding to the generalized gravitational force vector. $F_d \in \Re^m$ is given as

$$F_d = \begin{bmatrix} D(\dot{q}_p - \dot{\varphi}) \\ 0 \end{bmatrix}, \tag{9}$$

where $D \in \Re^{n\times n}$ includes the damping constants of the independent joints and is given as

$$D = \begin{bmatrix} d_1 & & 0 \\ & \ddots & \\ 0 & & d_n \end{bmatrix}. \tag{10}$$

Similarly $F_k \in \Re^m$ is given as

$$F_k = \begin{bmatrix} K(q_p - \varphi) \\ 0 \end{bmatrix}, \tag{11}$$

where $K \in \Re^{n\times n}$ includes the spring constants of the independent joints and is given as

$$K = \begin{bmatrix} k_1 & & 0 \\ & \ddots & \\ 0 & & k_n \end{bmatrix}. \tag{12}$$

$J^T(q)\lambda$ is the generalized constraint force vector and $\lambda \in \Re^{m-n}$ includes the Lagrange multipliers, i.e. the constraint forces imposed on the links that are disconnected to obtain an unconstrained system. $I^r \in \Re^{n\times n}$ includes the inertial parameters of the rotors and is given as

$$I^r = \begin{bmatrix} I_1^r r_1^2 & & 0 \\ & \ddots & \\ 0 & & I_n^r r_n^2 \end{bmatrix}, \tag{13}$$

where I_i^r is the moment of inertia of the ith rotor about its rotation axis. $u \in \Re^n$ includes the control torques after speed reduction.

Velocity-level constraint equations are subdivided into 2 subvectors as follows:

$$\begin{bmatrix} J_p & J_s \end{bmatrix} \begin{bmatrix} \dot{q}_p \\ \dot{q}_s \end{bmatrix} = 0, \tag{14}$$

where $J_p \in \Re^{(m-n)\times n}$ is the influence coefficient matrix of independent joint variables and $J_s \in \Re^{(m-n)\times(m-n)}$ is the influence coefficient matrix of dependent joint variables. As long as $\det(J_s) \neq 0$, i.e. in the absence of any drive (actuation) singularity, using Eq. (14) $\dot{q}_s$ can be written as

$$\dot{q}_s = -J_s^{-1} J_p \dot{q}_p. \tag{15}$$

Differentiation of Eq. (14) and then substitution of Eq. (15) into the resulting equation gives $\ddot{q}_s$ as follows:

$$\ddot{q}_s = -J_s^{-1}\left[J_p\ddot{q}_p + \left(\dot{J}_p - \dot{J}_s J_s^{-1} J_p\right)\dot{q}_p\right]. \tag{16}$$

M, **C**, and **G** can be subdivided into submatrices with respect to the independent and dependent joint variables to which they correspond as follows:

$$M = \begin{bmatrix} M_{pp} & M_{ps} \\ M_{sp} & M_{ss} \end{bmatrix}, \tag{17}$$

$$C = \begin{bmatrix} C_{pp} & C_{ps} \\ C_{sp} & C_{ss} \end{bmatrix}, \tag{18}$$

$$G = \begin{bmatrix} G_{pp} \\ G_{sp} \end{bmatrix}. \tag{19}$$

Therefore, Eq. (7) can be represented in 2 parts, as follows:

$$M_{pp}\ddot{q}_p + M_{ps}\ddot{q}_s + C_{pp}\dot{q}_p + C_{ps}\dot{q}_s + G_{pp}q_p + D\left(\dot{q}_p - \dot{\varphi}\right) + K\left(q_p - \varphi\right) - J_p^T\lambda = 0, \tag{20}$$

$$M_{sp}\ddot{q}_p + M_{ss}\ddot{q}_s + C_{sp}\dot{q}_p + C_{ss}\dot{q}_s + G_{sp}q_p - J_s^T\lambda = 0. \tag{21}$$

λ is obtained from Eq. (21) and then it is substituted into Eq. (20). After that, Eqs. (15) and (16) are substituted into the resulting equation. This gives the following n − dimensional dynamic equation:

$$N\ddot{q}_p + V\dot{q}_p - D\dot{\varphi} + Eq_p - K\varphi = 0, \tag{22}$$

where

$$N = M_{pp} - M_{ps}J_s^{-1}J_p - J_p^T\left(J_s^T\right)^{-1}\left(M_{sp} - M_{ss}J_s^{-1}J_p\right), \tag{23}$$

$$\begin{aligned} V \;=\; & -M_{ps}J_s^{-1}\left(\dot{J}_p - \dot{J}_s J_s^{-1}J_p\right) + C_{pp} - C_{ps}J_s^{-1}J_p + D - J_p^T\left(J_s^T\right)^{-1}\left[-M_{ss}J_s^{-1}\left(\dot{J}_p - \dot{J}_s J_s^{-1}J_p\right)\right. \\ & \left. + C_{sp} - C_{ss}J_s^{-1}J_p\right], \end{aligned} \tag{24}$$

$$E = K + G_{pp} - J_p^T\left(J_s^T\right)^{-1}G_{sp}. \tag{25}$$

Thus, the dynamics of the parallel manipulator can be written in augmented form by using Eqs. (22) and (8) as follows.

$$\begin{bmatrix} N & 0 \\ 0 & I^r \end{bmatrix}\begin{bmatrix} \ddot{q}_p \\ \ddot{\varphi} \end{bmatrix} + \begin{bmatrix} V & -D \\ -D & D \end{bmatrix}\begin{bmatrix} \dot{q}_p \\ \dot{\varphi} \end{bmatrix} + \begin{bmatrix} E & -K \\ -K & K \end{bmatrix}\begin{bmatrix} q_p \\ \varphi \end{bmatrix} = \begin{bmatrix} 0 \\ u \end{bmatrix} \tag{26}$$

As seen from Eq. (26), Lagrange multipliers are eliminated and dependent joint variables are not seen explicitly in the dynamics of the parallel manipulator. $\ddot{q}_p$ and $\ddot{\varphi}$ are extracted from Eq. (26) as follows:

$$\begin{bmatrix} \ddot{q}_p \\ \ddot{\varphi} \end{bmatrix} = \begin{bmatrix} A_V & C_V \\ B_V & D_V \end{bmatrix}\begin{bmatrix} \dot{q}_p \\ \dot{\varphi} \end{bmatrix} + \begin{bmatrix} A_E & C_E \\ B_E & D_E \end{bmatrix}\begin{bmatrix} q_p \\ \varphi \end{bmatrix} + \begin{bmatrix} C_T \\ D_T \end{bmatrix}u, \tag{27}$$

where

$$\begin{bmatrix} A_V & C_V \\ B_V & D_V \end{bmatrix} = -\begin{bmatrix} N & 0 \\ 0 & I^r \end{bmatrix}^{-1} \begin{bmatrix} V & -D \\ -D & D \end{bmatrix}, \tag{28}$$

$$\begin{bmatrix} A_E & C_E \\ B_E & D_E \end{bmatrix} = -\begin{bmatrix} N & 0 \\ 0 & I^r \end{bmatrix}^{-1} \begin{bmatrix} E & -K \\ -K & K \end{bmatrix}, \tag{29}$$

$$\begin{bmatrix} A_T & C_T \\ B_T & D_T \end{bmatrix} = \begin{bmatrix} N & 0 \\ 0 & I^r \end{bmatrix}^{-1}. \tag{30}$$

Hence, the state-space representation of the dynamics of the parallel manipulator can be obtained as

$$\dot{x}(t) = A(x)\, x(t) + B(x)\, u(t), \tag{31}$$

where $x \in \Re^{4n}$ is the state vector, $A \in \Re^{4n \times 4n}$ is the system matrix, $B \in \Re^{4n \times n}$ is the control input matrix, and $u \in \Re^n$ is the control vector. $\mathbf{x}$, $\mathbf{A}$, and $\mathbf{B}$ are defined as follows.

$$x = \begin{bmatrix} q_p \\ \dot{q}_p \\ \varphi \\ \dot{\varphi} \end{bmatrix} \tag{32}$$

$$A = \begin{bmatrix} 0 & I & 0 & 0 \\ A_E & A_V & C_E & C_V \\ 0 & 0 & 0 & I \\ B_E & B_V & D_E & D_V \end{bmatrix} \tag{33}$$

$$B = \begin{bmatrix} 0 \\ C_T \\ 0 \\ D_T \end{bmatrix} \tag{34}$$

End effector position and orientation can be represented in terms of manipulator joint variables as follows.

$$L_i = \gamma_i(\theta_1, \ldots, \theta_m) = 0 \quad i = 1, \ldots, n \tag{35}$$

Differentiation of the above equation gives

$$\dot{L} = J_m(q)\, \dot{q}, \tag{36}$$

where $J_m \in \Re^{n \times m}$ is the manipulator Jacobian matrix with

$$J_{m_{ij}} = \frac{\partial \gamma_i}{\partial q_j} \quad i = 1, \ldots, n, \quad j = 1, \ldots, m. \tag{37}$$

As long as $\det(J_c) \neq 0$, i.e. in the absence of any kinematic singularity, $\dot{q}$ can be expressed in terms of $\dot{L}$ by augmenting Eqs. (5) and (36) as follows:

$$\dot{q} = J_c^{-1} h, \tag{38}$$

where $J_c \in \Re^{m \times m}$ is

$$J_c = \begin{bmatrix} J \\ J_m \end{bmatrix} \tag{39}$$

and **h** is given as

$$h = \begin{bmatrix} 0 \\ \dot{L} \end{bmatrix}. \tag{40}$$

3. SDRE control

In recent years, the SDRE technique has been effectively used in the design of nonlinear controllers, observers, and filters due to its flexible design property, simplicity, and real-time implementation capability. The method is also called the frozen Riccati equation technique. In this method, first, the nonlinear system is represented in a state-dependent coefficient (SDC) form having a linear structure. An algebraic Riccati equation (ARE) is then formed using SDC matrices and state-dependent weighting coefficients. Therefore, the solution of the ARE is also state-dependent. Finally, suboptimum control inputs minimizing the performance index are obtained. The nonuniqueness of the SDC form and weighting coefficients give design flexibility and they are used to improve the performance of the controller. On the other hand, since the solution of a Hamilton–Jacobi–Bellman (HJB) partial differential equation (PDE) or a nonlinear two-point boundary value problem (TPBVP) is not needed, the method is simple as far as the computational burden is considered. In addition to these points, the algebraic SDRE depends on the current state and therefore control inputs can be implemented in real time.

3.1. SDRE nonlinear regulator problem

Consider an infinite-time nonlinear regulator problem. Minimize the following nonlinear cost functional non-quadratic in **x** but quadratic in **u**:

$$PI = \frac{1}{2}\int_{t_0}^{\infty} \left\{ x^T(t)\, Q(x)\, x(t) + u^T(t)\, R(x)\, u(t) \right\} dt \tag{41}$$

with respect to $x(t)$ and $u(t)$ subject to the full-state observable nonlinear system, having dynamics

$$\dot{x}(t) = f(x) + B(x)\, u(t), \quad x(t_0) = x_0 \tag{42}$$

in order to keep state $x(t)$ near zero and control $u(t)$ at minimum level. In the above equations, $Q(x) \in \Re^{s\times s}$ is the state weighting matrix satisfying $Q(x) = Q^T(x) \geq 0$, $R(x) \in \Re^{n\times n}$ is the input weighting matrix satisfying $R(x) = R^T(x) > 0$, $x(t) \in \Re^{4n}$ is the state vector, and $u(t) \in \Re^n$ is the control vector. It is assumed that $f(x)$ is a continuously differentiable function of **x**, $f(0) = 0$, and $B(x) \neq 0$. The nonlinear system of Eq. (42) can be rewritten in linear structure using SDC form:

$$\dot{x}(t) = A(x)\, x(t) + B(x)\, u(t) \quad x(t_0) = x_0 \ . \tag{43}$$

SDC form is not unique and SDC form should be chosen in such a way that $\left\{Q^{1/2}(x), A(x)\right\}$ and $\{A(x), B(x)\}$ are pointwise detectable and pointwise stabilizable, respectively [3,6,33]. If the state-dependent controllability matrix has full rank, the stabilizability condition is satisfied. Similarly, if the state-dependent observability matrix has full rank, the detectability condition is satisfied. Detectability condition is always satisfied by taking $\mathbf{Q}(\mathbf{x})$ as positive definite. As a result of this, the nonlinear control is obtained as

$$u(t) = -R^{-1}(x)\, B^T(x)\, P(x)\, x, \tag{44}$$

where $P(x)$ is obtained from the solution of algebraic SDRE:

$$P(x)A(x)+A^T(x)P(x)-P(x)B(x)R^{-1}(x)B^T(x)P(x)+Q(x)=0 \tag{45}$$

to get $P \geq 0$.

The SDRE method for the infinite-time nonlinear regulator problem is locally asymptotically stable and locally asymptotically optimal. The related theorems are given in [3,4,34].

In the SDRE method, in general, a nonlinear system is represented with different linear time-invariant systems as a result of the frozen nonlinear system at each point (or state). Therefore, the infinite-time nonlinear regulator problem is transformed into infinite-time linear quadratic regulator problems corresponding to the frozen nonlinear system at each point. This means that successive solutions of the linear quadratic regulator problem corresponding to the successive frozen nonlinear system approximate the solution of the SDRE nonlinear regulator problem for the whole states.

3.2. SDRE nonlinear tracking problem

Consider an infinite-time nonlinear tracking problem. Minimize the following nonlinear cost functional non-quadratic in **x** but quadratic in **u**:

$$PI=\frac{1}{2}\int_{t_0}^{\infty}\left\{e^T(t)Q(x)e(t)+u^T(t)R(x)u(t)\right\}dt, \tag{46}$$

$$e(t)=z(t)-y(t), \tag{47}$$

with respect to $e(t)$ and $u(t)$ subject to the full-state observable nonlinear system, having dynamics

$$\begin{aligned}\dot{x}(t)&=f(x)+B(x)u(t), \quad x(t_0)=x_0\\ y(t)&=g(x)\end{aligned} \tag{48}$$

in order to keep output $y(t)$ near desired output $z(t)$ and control $u(t)$ at minimum level. In the above equations, $Q(x)\in\Re^{s\times s}$ is the state weighting matrix satisfying $Q(x)=Q^T(x)\geq 0$, $R(x)\in\Re^{n\times n}$ is the input weighting matrix satisfying $R(x)=R^T(x)>0$, $e(t)$ is the error vector, $u(t)\in\Re^n$ is the control vector, $z(t)$ is the desired output vector, and $y(t)\in\Re^s$ is the output vector. It is assumed that $f(x)$ is a continuously differentiable function of **x**, $f(0)=0$, and $B(x)\neq 0$.

The SDRE technique has been essentially used for the infinite-time nonlinear regulator problem. Clouter and Stansbery [35] extended this technique for the nonlinear tracking problem. However, the extended technique increased the number of states variables. This leads to the need for more computation time. If the final time is large enough, an alternative method for the infinite-time nonlinear approximate optimal tracking problem is presented by using the SDC form of the nonlinear dynamics as follows:

i) Transform the nonlinear dynamics to SDC form

$$\begin{aligned}\dot{x}(t)&=A(x)x(t)+B(x)u(t), \quad x(t_0)=x_0\\ y(t)&=H(x)x(t)\end{aligned} \tag{49}$$

Since the SDC form is not unique, it should be chosen in such a way that $\left\{Q^{1/2}(x),A(x)\right\}$ and $\{A(x),B(x)\}$ are pointwise detectable and pointwise stabilizable, respectively.

ii) Obtain the solution of the SDRE

$$H^T(x)\,Q(x)\,H(x) + P(x)\,A(x) + A^T(x)\,P(x) - P(x)\,B(x)\,R^{-1}(x)\,B^T(x)\,P(x) = 0 \tag{50}$$

to get $P \geq 0$

iii) Calculate the linear vector equation

$$s(x) = \left(\left[A(x) - B(x)\,R^{-1}(x)\,B^T(x)\,P(x)\right]^T\right)^{-1} H^T(x)\,Q(x)\,z(t) \tag{51}$$

iv) Form the nonlinear controller

$$u(x) = -R^{-1}(x)\,B^T(x)\,[P(x)\,x(t) - s(x)] \tag{52}$$

4. Numerical example

As an example, a planar parallel manipulator used in [30] is taken into consideration to show the effectiveness of the SDRE method for the control of parallel robots having elastic joints (Figure 1). It is a 2-RRR parallel manipulator with 3 degrees of freedom. It is assumed that joints K, L, and M are driven by the motors. Rotation of the actuators is perpendicular to the plane of motion and the gravitational acceleration acts in $-y$ direction.

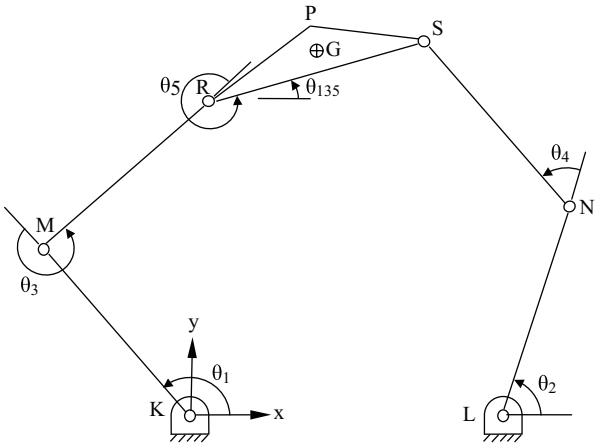

Figure 1. 2-RRR parallel manipulator.

The parallel manipulator is converted into 2 open kinematic chains by removing the joint at point S. The manipulator joint variables can then be written as

$$q = \begin{bmatrix} \theta_1 \\ \theta_2 \\ \theta_3 \\ \theta_4 \\ \theta_5 \end{bmatrix}. \tag{53}$$

The actuator variables are expressed as

$$\varphi = \begin{bmatrix} \varphi_1 \\ \varphi_2 \\ \varphi_3 \end{bmatrix}. \tag{54}$$

Eq. (53) can be partitioned as follows:

$$q_p = \begin{bmatrix} \theta_1 \\ \theta_2 \\ \theta_3 \end{bmatrix}, \tag{55}$$

$$q_s = \begin{bmatrix} \theta_4 \\ \theta_5 \end{bmatrix}, \tag{56}$$

where q_p is the vector of independent joint variables and q_s is the vector of dependent joint variables.

Two constraint equations are written associated with the removal of the joint at point S. At the position level, these constraint equations can be written as

$$a_1 c\theta_1 + a_3 c\theta_{13} + a_5 c\theta_{135} - a_2 c\theta_2 - a_4 c\theta_{24} - b_1 = 0, \tag{57}$$

$$a_1 s\theta_1 + a_3 s\theta_{13} + a_5 s\theta_{135} - a_2 s\theta_2 - a_4 s\theta_{24} = 0, \tag{58}$$

where the lengths are represented as $KM = a_1$, $LN = a_2$, $MR = a_3$, $NS = a_4$, $RS = a_5$, and $KL = b_1$. Angle combinations are denoted as $\theta_{ijk} = \theta_i + \theta_j + \theta_k$. $c(\cdot) = \cos(\cdot)$, and $s(\cdot) = \sin(\cdot)$.

When the equations of motion of the parallel manipulator are obtained in SDC form, the nonzero entries of matrices **M**, **C**, **G**, and **J** in Eq. (7) are as follows.

$$\begin{aligned} M(1,1) \;=\; & m_1 \tfrac{a_1^2}{4} + I_{1zz} + m_3 a_1^2 + m_3 a_1 a_3 c\theta_3 + m_3 \tfrac{a_3^2}{4} + I_{3zz} + m_5 a_1^2 + m_5 a_3^2 + m_5 c_5^2 + I_{5zz} \\ & + 2m_5 a_1 a_3 c\theta_3 + 2m_5 a_1 c_5 c(\theta_{35} + \kappa) + 2m_5 a_3 c_5 c(\theta_5 + \kappa) + m_3^A a_1^2 + I_{3zz}^r \end{aligned} \tag{59}$$

$$M(1,3) = \frac{1}{2} m_3 a_1 a_3 c\theta_3 + m_3 \frac{a_3^2}{4} + I_{3zz} + m_5 a_3^2 + m_5 c_5^2 + I_{5zz}$$

$$+ m_5 a_1 a_3 c\theta_3 + m_5 a_1 c_5 c(\theta_{35} + \kappa) + 2m_5 a_3 c_5 c(\theta_5 + \kappa) \tag{60}$$

$$M(1,5) = m_5 c_5^2 + I_{5zz} + m_5 a_1 c_5 c(\theta_{35} + \kappa) + m_5 a_3 c_5 c(\theta_5 + \kappa) \tag{61}$$

$$M(2,2) = m_2 \frac{a_2^2}{4} + I_{2zz} + m_4 a_2^2 + m_4 a_2 a_4 c\theta_4 + m_4 \frac{a_4^2}{4} + I_{4zz} \tag{62}$$

$$M(2,4) = \frac{1}{2} m_4 a_2 a_4 c\theta_4 + m_4 \frac{a_4^2}{4} + I_{4zz} \tag{63}$$

$$M(3,3) = m_3 \frac{a_3^2}{4} + I_{3zz} + m_5 a_3^2 + m_5 c_5^2 + I_{5zz} + 2m_5 a_3 c_5 c(\theta_5 + \kappa) \tag{64}$$

$$M(3,5) = m_5 c_5^2 + I_{5zz} + m_5 a_3 c_5 c(\theta_5 + \kappa) \tag{65}$$

$$M(4,4) = m_4 \frac{a_4^2}{4} + I_{4zz} \tag{66}$$

$$M(5,5) = m_5 c_5^2 + I_{5zz} \tag{67}$$

$$C(3,1) = \left[\frac{1}{2} m_3 a_1 a_3 s\theta_3 + m_5 a_1 a_3 s\theta_3 + m_5 a_1 c_5 s(\theta_{35} + \kappa) \right] \dot{\theta}_1 \tag{68}$$

$$C(3,3) = \left[\frac{1}{2} m_3 a_1 a_3 s\theta_3 + m_5 a_1 a_3 s\theta_3 + m_5 a_1 c_5 s(\theta_{35} + \kappa) \right] \dot{\theta}_1 \tag{69}$$

$$C\left(3,5\right)=\left[m_5a_1c_5s\left(\theta_{35}+\kappa\right)\right]\dot{\theta}_1 \tag{70}$$

$$C\left(4,2\right)=\left(\frac{1}{2}m_4a_2a_4s\theta_4\right)\dot{\theta}_2 \tag{71}$$

$$C\left(4,4\right)=\left(\frac{1}{2}m_4a_2a_4s\theta_4\right)\dot{\theta}_2 \tag{72}$$

$$C\left(5,1\right)=\left[m_5a_1c_5s\left(\theta_{35}+\kappa\right)+m_5a_3c_5s\left(\theta_5+\kappa\right)\right]\dot{\theta}_1 \tag{73}$$

$$C\left(5,3\right)=\left[m_5a_1c_5s\left(\theta_{35}+\kappa\right)+2m_5a_3c_5s\left(\theta_5+\kappa\right)\right]\dot{\theta}_1+\left[m_5a_3c_5s\left(\theta_5+\kappa\right)\right]\dot{\theta}_3 \tag{74}$$

$$C\left(5,5\right)=\left[m_5a_1c_5s\left(\theta_{35}+\kappa\right)+m_5a_3c_5s\left(\theta_5+\kappa\right)\right]\dot{\theta}_1+\left[m_5a_3c_5s\left(\theta_5+\kappa\right)\right]\dot{\theta}_3 \tag{75}$$

$$G\left(1,1\right)=\left(m_1\frac{a_1}{2}\frac{c\theta_1}{\theta_1}+m_3a_1\frac{c\theta_1}{\theta_1}+m_5a_1\frac{c\theta_1}{\theta_1}+m_3^Aa_1\frac{c\theta_1}{\theta_1}\right)g \tag{76}$$

$$G\left(1,3\right)=\left(m_3\frac{a_3}{2}\frac{c\theta_{13}}{\theta_3}+m_5a_3\frac{c\theta_{13}}{\theta_3}+m_5c_5\frac{c\left(\theta_{135}+\kappa\right)}{\theta_3}\right)g \tag{77}$$

$$G\left(2,2\right)=\left(m_2\frac{a_2}{2}\frac{c\theta_2}{\theta_2}+m_4a_2\frac{c\theta_2}{\theta_2}+m_4\frac{a_4}{2}\frac{c\theta_{24}}{\theta_2}\right)g \tag{78}$$

$$G\left(3,3\right)=\left(m_3\frac{a_3}{2}\frac{c\theta_{13}}{\theta_3}+m_5a_3\frac{c\theta_{13}}{\theta_3}+m_5c_5\frac{c\left(\theta_{135}+\kappa\right)}{\theta_3}\right)g \tag{79}$$

$$G\left(4,2\right)=\left(m_2\frac{a_2}{2}\frac{c\theta_2}{\theta_2}+m_4a_2\frac{c\theta_2}{\theta_2}+m_4\frac{a_4}{2}\frac{c\theta_{24}}{\theta_2}\right)g \tag{80}$$

$$G\left(5,3\right)=\left(m_5c_5\frac{c\left(\theta_{135}+\kappa\right)}{\theta_3}\right)g \tag{81}$$

$$J\left(1,1\right)=-a_1s\theta_1-a_3s\theta_{13}-a_5s\theta_{135} \tag{82}$$

$$J\left(1,2\right)=a_2s\theta_2+a_4s\theta_{24} \tag{83}$$

$$J\left(1,3\right)=-a_3s\theta_{13}-a_5s\theta_{135} \tag{84}$$

$$J\left(1,4\right)=a_4s\theta_{24} \tag{85}$$

$$J\left(1,5\right)=-a_5s\theta_{135} \tag{86}$$

$$J\left(2,1\right)=a_1c\theta_1+a_3c\theta_{13}+a_5c\theta_{135} \tag{87}$$

$$J\left(2,2\right)=-a_2c\theta_2-a_4c\theta_{24} \tag{88}$$

$$J\left(2,3\right)=a_3c\theta_{13}+a_5c\theta_{135} \tag{89}$$

$$J\left(2,4\right)=-a_4c\theta_{24} \tag{90}$$

$$J\left(2,5\right)=a_5c\theta_{135} \tag{91}$$

Here, m_i, $i=1,\ldots,5$ is the mass of link i; m_3^A is the total mass of the actuator and the gear box on link 1; I_i, $i=1,\ldots,5$ is the moment of inertia of link i with respect to the center of mass of link i; I_i^r, $i=1,\ldots,3$ is the moment of inertia of the rotor i with respect to its rotation axis; and length $c_5=RG$ and angle $\kappa=\angle GRS$.

The position of point P and orientation of the moving platform can be written as

$$x_p = a_1 c\theta_1 + a_3 c\theta_{13} + b_5 c\left(\theta_{135} + \gamma\right), \tag{92}$$

$$y_p = a_1 s\theta_1 + a_3 s\theta_{13} + b_5 s\left(\theta_{135} + \gamma\right), \tag{93}$$

$$\theta_{135} = \theta_1 + \theta_3 + \theta_5, \tag{94}$$

where length $b_5 = RP$ and angle $\gamma = \angle PRS$.

The nonzero entries of the matrix $\mathbf{J}_m$ in Eq. (36) are as follows.

$$J_m\left(1,1\right) = -a_1 s\theta_1 - a_3 s\theta_{13} - b_5 s\left(\theta_{135} + \gamma\right) \tag{95}$$

$$J_m\left(1,3\right) = -a_3 s\theta_{13} - b_5 s\left(\theta_{135} + \gamma\right) \tag{96}$$

$$J_m\left(1,5\right) = -b_5 s\left(\theta_{135} + \gamma\right) \tag{97}$$

$$J_m\left(2,1\right) = a_1 c\theta_1 + a_3 c\theta_{13} + b_5 c\left(\theta_{135} + \gamma\right) \tag{98}$$

$$J_m\left(2,3\right) = a_3 c\theta_{13} + b_5 c\left(\theta_{135} + \gamma\right) \tag{99}$$

$$J_m\left(2,5\right) = b_5 c\left(\theta_{135} + \gamma\right) \tag{100}$$

$$J_m\left(3,1\right) = 1 \tag{101}$$

$$J_m\left(3,3\right) = 1 \tag{102}$$

$$J_m\left(3,5\right) = 1 \tag{103}$$

The geometric data and the mass, inertial properties, and gear ratios used in the simulations are as follows: a_i = 0.5 m, $i = 1,\ldots,5$, b_1 = 0.8 m, b_5 = 0.3 m, c_5 = 0.25 m, γ = 20 deg, κ = 7 deg, $m_i = 3$ kg, $i = 1,\ldots,4$, and $m_5 = 4$ kg. Links 1, 2, 3, and 4 are assumed to be uniform. Dimensions of the actuator and gear boxes are small relative to the dimensions of the links. $m_3^A = 0.5$ kg, $I_1^r = 7 \times 10^{-5}$ kgm^2, $I_2^r = 8 \times 10^{-5}$ kgm^2, $I_3^r = 9 \times 10^{-5}$ kgm^2, $r_i = 100$, $i = 1,2,3$. Torsional stiffness coefficients are taken as $k_i = 5000$ Nm/rad, $i = 1,2,3$. A 3% damping ratio is considered for rotors. Therefore, structural damping coefficients are taken as d_1 = 0.0355 Nms/rad, d_2 = 0.0379 Nms/rad, and d_3 = 0.0402 Nms/rad. The reference motion of the position of point P and the orientation of the moving platform are given as

$$x_p^r\left(t\right) = \begin{cases} 0.25 + \frac{0.3}{T}\left[t - \frac{T}{2\pi}\sin\left(\frac{2\pi}{T}t\right)\right] \ m & 0 \le t \le T \\ 0.55 \ m & t > T \end{cases}, \tag{104}$$

$$y_p^r\left(t\right) = \begin{cases} 0.90 - \frac{0.3}{T}\left[t - \frac{T}{2\pi}\sin\left(\frac{2\pi}{T}t\right)\right] \ m & 0 \le t \le T \\ 0.60 \ m & t > T \end{cases}, \tag{105}$$

$$\theta_{135}^r\left(t\right) = \begin{cases} 15 + \frac{15}{T}\left[t - \frac{T}{2\pi}\sin\left(\frac{2\pi}{T}t\right)\right] \ \text{deg} & 0 \le t \le T \\ 30 \ \text{deg} & t > T \end{cases}, \tag{106}$$

where T is the motion period. It is taken as 5 s. Therefore, the reference (desired output) vector will be

$$z(t) = \begin{bmatrix} x_p^r\left(t\right) \\ y_p^r\left(t\right) \\ \theta_{135}^r\left(t\right) \end{bmatrix}. \tag{107}$$

Initial values for the positions of the independent joints are taken as $\theta_{1i} = 135$ deg, $\theta_{2i} = 85$ deg, and $\theta_{3i} =$ –90 deg. Therefore, initial values for the positions of the dependent joints are calculated as $\theta_{4i} = 51.44$ deg, $\theta_{5i} =$ –29.27 deg. These initial joint angular positions lead to the initial position of point P and orientation of the moving platform as $x_{pi} = 0.2501$ m, $y_{pi} = 0.8729$ m, $\theta_{135i} = 13.5400$ deg. Initially, the system is at rest.

The Runge–Kutta fourth-order numerical integration method is used to solve the ordinary differential equations that describe the dynamics of the system. Computer codes are written in MATLAB. In the simulations, the sampling time step is taken as 0.01 s. As far as the initial actual and reference values of the position of point P and orientation of the moving platform are considered, it is seen that the manipulator begins its motion with initial misposition and misorientation.

The weighting coefficients in the performance index are taken as $Q = \begin{bmatrix} 3 \times 10^4 I_3 & 0 \\ 0 & I_3 \end{bmatrix}$ and $R = I_3$. The point P position and moving platform orientation are given in Figures 2–4. The deflections and actuator torques are presented in Figures 5 and 6. The simulation results indicate that satisfactory tracking accuracies are obtained both in the position of point P and orientation of the moving platform. The maximum position tracking errors after settling the trajectory are 6.4148×10^{-4} m and -1.0342×10^{-3} m in horizontal and vertical directions, respectively. The maximum orientation tracking error after settling the trajectory is 0.0421 deg. Final position errors are -5.5811×10^{-5} m and -4.8338×10^{-4} m in horizontal and vertical directions, respectively. Final orientation error is 7.4787×10^{-3} deg. Furthermore, maximum start-up torque is in the order of 70 Nm.

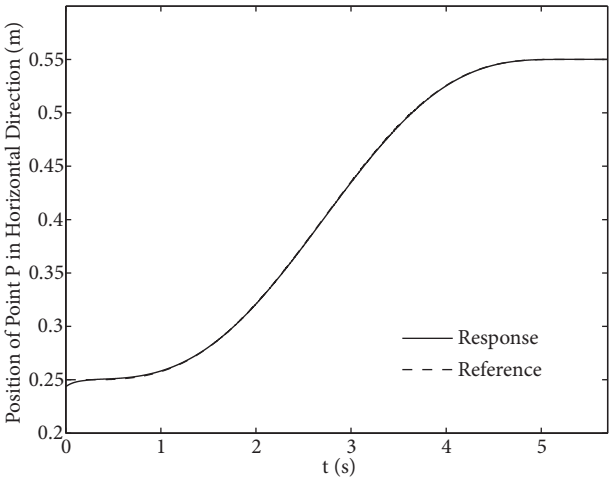

Figure 2. Position of point P in horizontal direction.

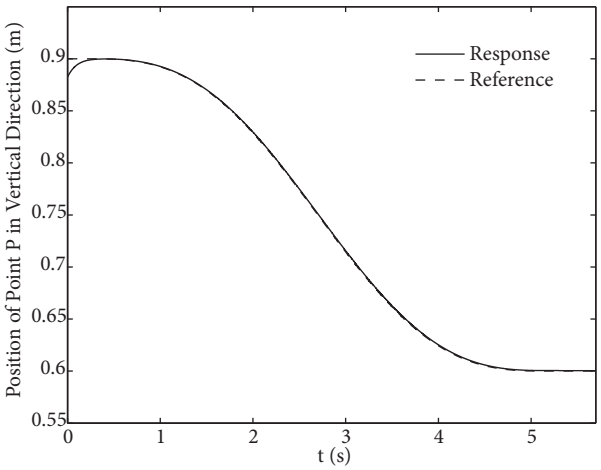

Figure 3. Position of point P in vertical direction.

The control simulations are repeated by taking the robot inertia and elastic parameters 10% smaller in the dynamic equations for the examination of modeling error. In this case, the weighting coefficients are taken as $Q = \begin{bmatrix} 5 \times 10^4 I_3 & 0 \\ 0 & I_3 \end{bmatrix}$ and $R = I_3$. The point P position and moving platform orientation are given in Figures 7–9. The deflections and actuator torques are presented in Figures 10 and 11. The maximum position tracking errors after settling the trajectory are 5.5602×10^{-4} m and -1.5532×10^{-3} m in horizontal and vertical directions, respectively. The maximum orientation tracking error after settling the trajectory is 0.0742 deg. Final position errors are -7.5572×10^{-5} m and -1.0111×10^{-3} m in horizontal and vertical directions,

respectively. Final orientation error is 0.057 deg. Furthermore, maximum start-up torque is in the order of 80 Nm. Tracking and steady state errors can be decreased much more by increasing **Q** at the expense of greater actuator torques.

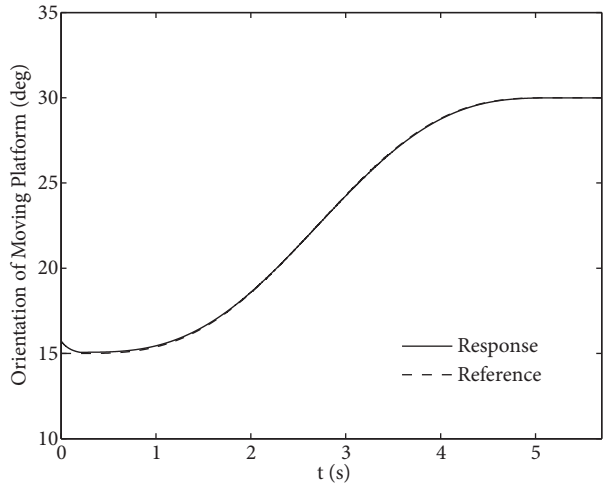

Figure 4. Orientation of moving platform.

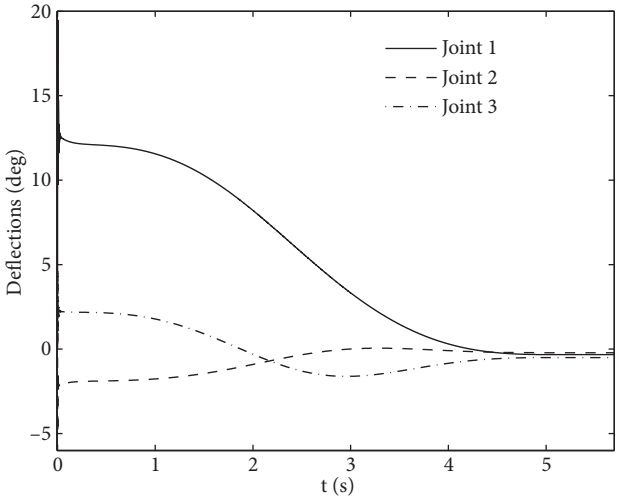

Figure 5. Deflections.

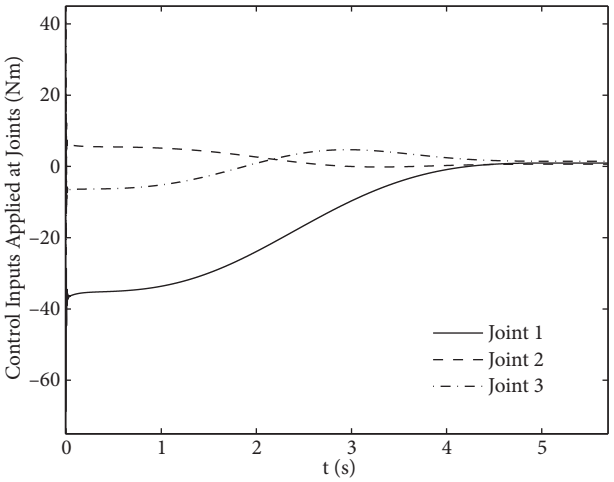

Figure 6. Control inputs applied at joints.

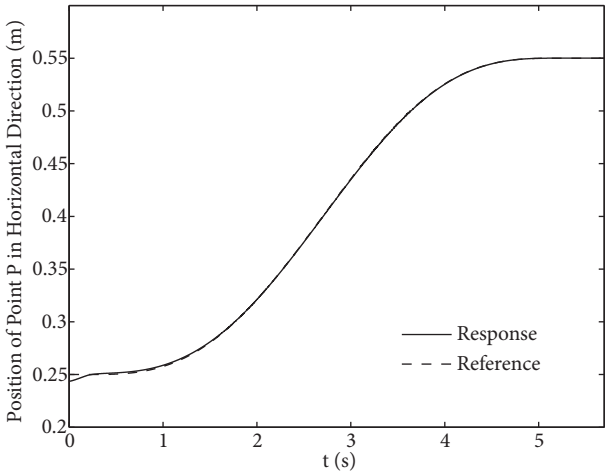

Figure 7. Position of point P in horizontal direction.

The detectability condition is ensured by taking **Q** as positive definite and the stabilizability condition is ensured by checking the state-dependent controllability matrix at each time step for both simulations.

5. Conclusions

This paper presents an algorithm based on the SDRE for the trajectory tracking control of parallel robots with elastic joints. Structural stiffness and damping characteristics of the joints are modeled as torsional springs and dampers, respectively. First, an unconstrained system obtained from the constrained system is considered and its dynamic equations are written. The constraint equations are then expressed. The first and second derivatives of dependent joint variables are represented in terms of independent joint variables by using the constraint equations. After that, by taking independent joint variables, actuator variables, and their first

derivatives as state variables, dynamic equations are expressed in state space form. Finally, the SDRE tracking control method is presented.

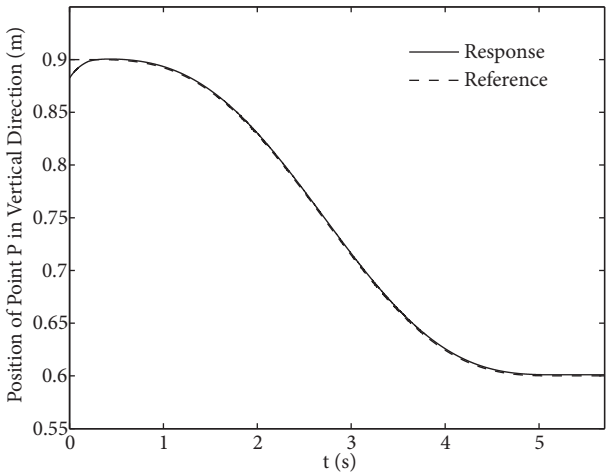

Figure 8. Position of point P in vertical direction.

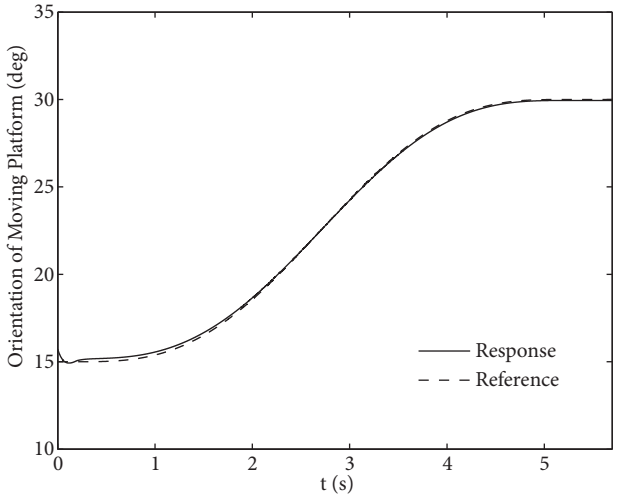

Figure 9. Orientation of moving platform.

In the SDRE method, first, the nonlinear system is represented in a SDC form having a linear structure. The ARE is then formed using SDC matrices and state-dependent weighting coefficients. Therefore, the solution of the ARE is also state-dependent. Finally, suboptimum control inputs minimizing the performance index are obtained. The nonuniqueness of the SDC form and weighting coefficients give design flexibility and they are used to improve the performance of the controller. On the other hand, since the solution of a HJB PDE or a nonlinear TPBVP is not needed, the method is simple as far as the computational burden is concerned. In addition, the algebraic SDRE depends on the current state, and therefore control inputs can be implemented in real time.

As a case study, a 2-RRR planar parallel manipulator is considered to illustrate the effectiveness of the SDRE method for the control of parallel robots having elastic joints. It is shown that parallel manipulators with significant joint flexibility can follow the specified trajectory with satisfactory performance by the proposed

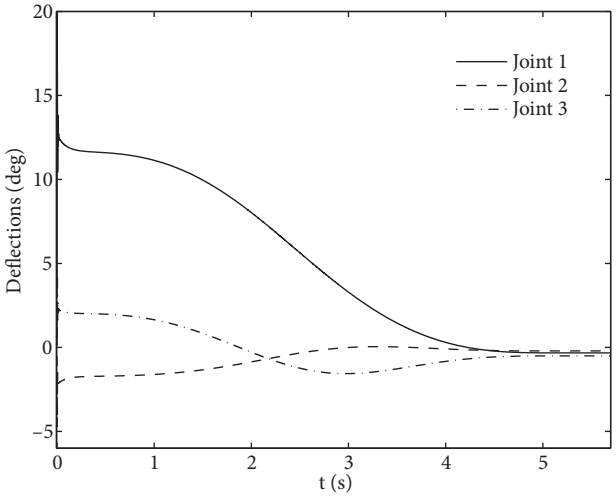

Figure 10. Deflections.

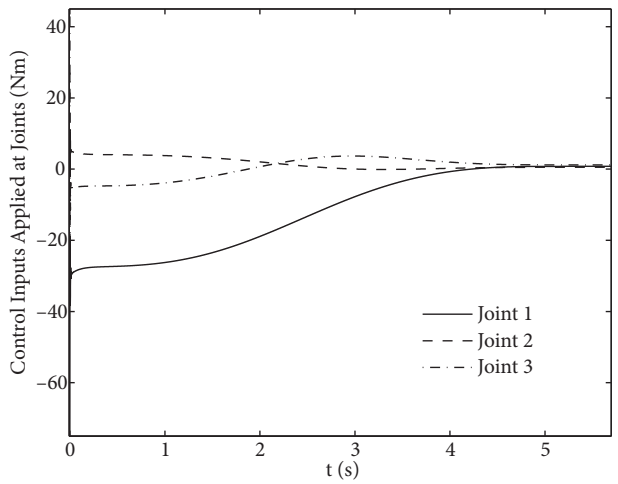

Figure 11. Control inputs applied at joints.

control algorithm. Simulations are performed in the presence of only initial error and no modeling error and in the presence of both initial error and modeling error. For the second simulation, mass/inertia parameters, spring and damping constants, are assumed to be 10% smaller in the model. Good tracking accuracies are obtained in both simulations as seen in Figures 2–4 and 7–9. The torques to be supplied by the actuators do not increase significantly when the modeling error is considered, as seen in Figures 6 and 11. In general, the tracking and steady-state errors are decreased by increasing weighting coefficients **Q** while the control torques are decreased by increasing weighting coefficients **R**.

References

[1] Rivin EI. Compliance breakdown for robot structures. In: Proceedings of Symposium Engineering Applications in Mechanics; June 1984; Toronto, Ontario Canada. pp. 55–67.

[2] Good MC, Sweet LM, Strobel, KL. Dynamic models for control system design of integrated robot and drive systems. J Dyn Syst-T ASME 1985; 107: 53–59.

[3] Cloutier JR, D'Souza CN, Mracek CP. Nonlinear regulation and nonlinear H_∞ control via the state-dependent Riccati equation technique: Part 1, Theory; Part 2, Examples. In: First International Conference on Nonlinear Problems in Aviation and Aerospace; 9–11 May 1996; Daytona Beach, FL, USA. pp. 117–141.

[4] Mracek CP, Cloutier JR. Control designs for the nonlinear benchmark problem via the state-dependent Riccati equation method. Int J Robust Nonlin 1998; 8: 401–433.

[5] Cloutier JR, Stansbery DT. The capabilities and art of state-dependent Riccati equation-based design. In: American Control Conference; 8–10 May 2002; Anchorage, AK, USA. pp. 86–91.

[6] Shamma JS, Cloutier JR. Existence of SDRE stabilizing feedback. IEEE T Automat Contr 2003; 48: 513–517.

[7] Cimen T. Systematic and effective design of nonlinear feedback controllers via the state-dependent Riccati equation (SDRE) method. Annu Rev Control 2010; 34: 32–51.

[8] Cimen T. Survey of state-dependent Riccati equation in nonlinear optimal feedback control synthesis. J Guid Control Dynam 2012; 35: 1025–1047.

[9] Erdem EB, Alleyne AG. Experimental real-time SDRE control of an underactuated robot. In: 40th IEEE Conference on Decision and Control; 4–7 December 2001; Piscataway, NJ, USA. pp. 219–224.

[10] Terashima S, Iwase M, Furuta K, Suzuki S, Hatakeyama S. A design of servo controller for nonlinear systems using state dependent Riccati equation. In: 42nd IEEE Conference on Decision and Control; 9–12 December 2003; Maui, HI, USA. pp. 3864–3869.

[11] Watanabe K, Iwase M, Hatakeyama S, Maruyama T. Control strategy for a snake-like robot based on constraint force and verification by experiment. In: IEEE/RSJ International Conference on Intelligent Robots and Systems; 22–26 September 2008; Nice, France. pp. 1618–1623.

[12] Nekoo SR. Nonlinear closed loop optimal control: a modified state-dependent Riccati equation. ISA T 2012; 52: 285–290.

[13] Cree AG, Damaren CJ. Causal approximate inversion for control of structurally flexible manipulators using nonlinear inner-outer factorization. J Robotic Syst 2001; 18: 391–399.

[14] Shawky A, Ordys A, Grimble MJ. End-point control of a flexible-link manipulator using H∞ nonlinear control via a state-dependent Riccati equation. In: International Conference on Control Applications; 18–20 September 2002; Glasgow, UK. pp. 501–506.

[15] Shawky AM, Ordys AW, Petropoulakis L, Grimble MJ. Position control of flexible manipulator using non-linear H∞ with state-dependent Riccati equation. P I Mech Eng I-J Sys 2007; 221: 475–486.

[16] Fenili A, Balthazar JM. The rigid-flexible nonlinear robotic manipulator: modeling and control. Commun Nonlinear Sci 2011; 16: 2332–2341.

[17] Korayem MH, Irani M, Nekoo SR. Load maximization of flexible joint mechanical manipulator using nonlinear optimal controller. Acta Astronaut 2011; 69: 458–469.

[18] Spong MW. Modeling and control of elastic joint robots. J Dyn Syst-T ASME 1987; 109: 310–319.

[19] Jankowski KP, Van Brussel H. An approach to discrete inverse dynamics control of flexible joint robots. IEEE J Robotic Autom 1992; 8: 651–658.

[20] Ider SK, Ozgoren MK. Trajectory tracking control of flexible joint robots. Computers and Structures 2000; 76: 757–763.

[21] Ghorbel F, Spong MW. Integral manifolds of singularly perturbed systems with application to rigid-link flexible-joint multibody systems. Int J Nonlin Mech 2000; 35: 133–155.

[22] Ider SK. Force and motion trajectory tracking control of flexible joint robots. Mech Mach Theory 2000; 35: 363–378.

[23] Hu YR, Vukovich G. Position and force control of flexible joint robots during constrained motion tasks. Mech Mach Theory 2001; 36: 853–871.

[24] M F, Wang DB. Hybrid force/position control scheme for flexible joint robot with friction between and the end-effector and the environment. Int J Eng Sci 2008; 46: 1266–1278.

[25] Chatlatanagulchai W, Meckl PH. Model-independent control of a flexible-joint robot manipulator. J Dyn Syst-T ASME 2009; 131: 041003.

[26] Jiang ZH, Higaki S. Control of flexible joint robot manipulators using a combined controller with neural network and linear regulator. P I Mech Eng I-J Sys 2011; 225: 798–806.

[27] Yoo SJ. Actuator fault detection and adaptive accommodation control of flexible-joint robots. IET Control Theory A 2012; 6: 1497–1507.

[28] Yena HM, Li THS, Chang YC. Adaptive neural network based tracking control for electrically driven flexible-joint robots without velocity measurements. Comput Math Appl 2012; 64: 1022–1032.

[29] Fateh MM. Nonlinear control of electrical flexible-joint robots. Nonlinear Dyn 2012; 67: 2549–2559.

[30] Ider SK, Korkmaz O. Trajectory tracking control of parallel robots in the presence of joint drive flexibility. J Sound Vib 2009; 319: 77–90.

[31] Ozgoli S, Taghirad HD. A survey on the control of flexible joint robots. Asian J Control 2006; 8: 1–15.

[32] Dwivedya SK, Eberhard P. Dynamic analysis of flexible manipulators, a literature review. Mech Mach Theory 2006; 41: 749–777.

[33] Kilicaslan S, Banks SP. Existence of solutions of Riccati differential equations. J Dyn Syst-T ASME 2012; 134: 031001.

[34] Banks HT, Lewis BM, Tran HT. Nonlinear feedback controllers and compensators: a state-dependent Riccati equation approach. Comput Optim Appl 2007; 37: 177–218.

[35] Cloutier JR, Stansbery DT. Nonlinear, hybrid bank-to-turn/skid-to-turn autopilot design. In: AIAA Guidance, Navigation, and Control Conference; 6–9 August 2001; Montreal, Canada.